INSTITUTE OF PHYSICS PUBLISHING JOURNAL OF PHYSICS D: APPLIED PHYSICS

J. Phys. D: Appl. Phys. **39** (2006) 1853–1865 doi:10.1088/0022-3727/39/9/021

Moment conserving method for modelling multiple collisions in particle simulations

F Iza and J K Lee[1]

Department of Electronic and Electrical Engineering, Pohang University of Science and Technology, Pohang 790-784, Republic of Korea

E-mail: jkl@postech.ac.kr

Received 16 February 2006, in final form 7 March 2006
Published 20 April 2006
Online at stacks.iop.org/JPhysD/39/1853

Abstract

A statistical procedure for modelling the cumulative effect of multiple collisions in particle simulations is presented. The procedure approximates the probability density function (PDF) of the final scattering angle and that of the particle net displacement by parametric functions. Formulae for determining the moments of the exact PDFs as a function of the statistics of a single collision event are derived. Using these formulae, the parametric functions can be fitted to yield the same first moments as the real distributions. Therefore, in contrast to other approaches where after one iteration the error in the first moments depends on the number of collisions modelled, the present model provides always the right moments. Correlation between the scattering angle and the displacement of the particle is also considered and enforced by means of a Gaussian copula.

(Some figures in this article are in colour only in the electronic version)

1. Introduction

Particle simulation [1] is a well-established technique for modelling physical systems in which particles are not in equilibrium and their kinetics are crucial for describing the behaviour of the system. One such system is the low-temperature plasma. Particle-in-cell (PIC) simulations of plasmas can capture kinetic effects that are not reproducible by means of widely used fluid models and they provide excellent agreement with experimental observations [2]. In this paper we consider collisions typically encountered in plasma simulations. The method for modelling the cumulative effect of multiple collisions, however, can be applied to particles undergoing multiple collisions in other systems, e.g. ions being implanted, particle detectors, etc. In fact, the treatment of multiple collisions was first applied to the study of particle penetration and diffusion in solids and has developed into the so-called condense-history Monte Carlo technique [3–7]. Only recently, schemes to handle multiple collisions in particle simulation of plasmas have been considered [8–10].

In a typical PIC Monte Carlo plasma simulation, the integration of the equations of motion and the simulation of collision events are decoupled and computed sequentially, i.e. in each time step, particles are first advanced in time and then undergo collisions [2,11]. The particles that collide are chosen randomly and their velocities are scattered according to the physics underlying the collision events. Therefore, the particle position is advanced deterministically based on the velocity at the end of the previous time step and in the presence of a collision the final velocity is scattered statistically. This model is valid only if the time step (Δt) used for the integration of the equations of motion is smaller than the time of fly between collisions, i.e. $\nu\Delta t \ll 1$ where ν is the collision frequency and Δt the simulation time step. When $\nu\Delta t \ll 1$, the probability of a particle undergoing more than one collision per time step is negligible and for those particles undergoing collisions it can be assumed, without incurring significant error, that the collision takes place at the end of the time step. For accuracy, $\nu\Delta t$ should be kept below 0.1.

The time step (Δt) in plasma simulations is typically set by stability and accuracy criteria dictated by the numerical method used for the integration of the equations of motion. For low-temperature low-pressure plasmas, the condition $\nu\Delta t \ll 1$ is typically satisfied. The fulfilment of this condition, however, is not guaranteed. When the time interval is constrained by the collision frequency instead of by other numerical or physical considerations (e.g. high density and high pressure plasmas),

[1] Author to whom any correspondence should be addressed.

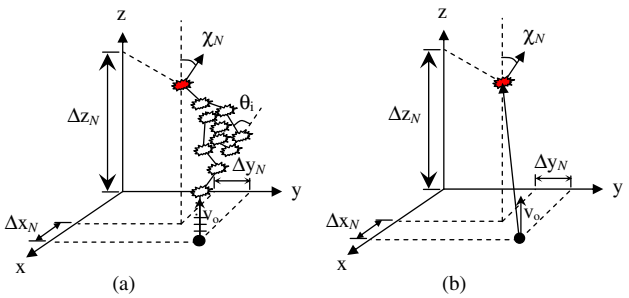

Figure 1. Advancing of a particle undergoing multiple collisions. (*a*) PIC–MCC approach in which $\nu\Delta t \ll 1$: each collision is modelled individually and several time steps are simulated in between collisions. (*b*) PIC–MCC approach in which $\nu\Delta t \gg 1$: the particle is directly positioned at the final position after N collisions and only the net displacement (Δx_N, Δy_N, Δz_N) and the cumulative scattering angle (χ_N) are computed.

modelling multiple collisions in one time step is desirable. This improves the speed of the simulation by allowing a larger time step, and by reducing the number of collisions that are simulated. Significant performance improvements were reported in [8] when modelling multiple Coulomb collisions in the study of various plasma problems.

The aim of this work is to develop a fictitious collision event that has a cross section such that the scattering of a particle due to one single fictitious collision has the same result as multiple physical collisions (figure 1). In figure 1 and throughout the manuscript θ_i represents the scattering angle of the ith collision; χ_N the cumulative scattering angle after N collisions and Δx_N, Δy_N and Δz_N, the net particle displacement in a Cartesian coordinate system after N collisions. It should be noted that χ_N is measured with respect to the initial particle velocity (assumed to be in the z direction) while θ_i is measured with respect to the particle velocity just before the ith collision. As a result of the multiple collisions, both the scattering angle and the particle position must be determined statistically. In this work, we use a geometrical analysis similar to that presented by Nanbu for modelling multiple small-angle collisions [8]. Here, we extend his work accounting for collisions with any scattering angle as well as for the position of the particles. Furthermore, the correlation between the scattering angle and the position of the particles is also considered in the analysis.

The rest of the manuscript is organized as follows. In section 2, a review of the modelling of single collisions in PIC codes is presented. In section 3, the statistics of a particle undergoing N collisions are derived and a scheme to model multiple collisions is introduced. Examples and comparisons with conventional PIC results are also presented to evaluate the accuracy of the method. Electrons undergoing small angle Coulomb collisions and large angle electron-neutral collisions are considered in the examples. Finally, further improvements of the simulation scheme are considered in section 4 and conclusions are drawn in section 5.

2. Particle-in-cell Monte Carlo simulation: treatment of one collision

In particle simulations, collisions are modelled using a Monte Carlo, i.e. statistical, procedure. Particles undergoing collisions are selected randomly and scattered taking into account the differential scattering cross section of the collision event [12]. The probability density function (PDF) of this single-event differential cross section is an input to the simulation and it is based on either theoretical calculations or experimental measurements. The scattering angle of a particle undergoing a single collision is determined by inverting the corresponding cumulative distribution function (CDF). This requires the generation of a random number (R) uniformly distributed between 0 and 1 and an analytical expression of the inverse CDF [11, 12]. Although other techniques such as the rejection method can be used to sample a distribution function, inverting the CDF is the preferred approach because it allows imposing a correlation between variables without the knowledge of the joint distribution function (as described in section 3.3).

Two types of physical collisions are considered in the examples presented in this paper. The first collision is the elastic scattering of electrons due to collisions with argon neutrals. Based on the differential cross section given by Surendra *et al* [13], the PDF and the inverse CDF of the cosine of the scattering angle after a single collision are

$$f(y=\cos\theta) = \frac{\varepsilon}{\ln(1+\varepsilon)}\frac{1}{2+\varepsilon(1-y)} \Leftrightarrow \cos\theta = \frac{2+\varepsilon-2(1+\varepsilon)^R}{\varepsilon}, \tag{1}$$

where ε is the energy of the colliding electron and R is a random number uniformly distributed between 0 and 1. The averages of the first three powers of the cosine of the scattering angle are

$$\begin{aligned}
\langle\cos\theta\rangle &= \int_{-1}^{1} y\, f(y)\,\mathrm{d}y = 1+\frac{2}{\varepsilon}-\frac{2}{\ln(1+\varepsilon)},\\
\langle\cos^2\theta\rangle &= \int_{-1}^{1} y^2\, f(y)\,\mathrm{d}y = 1+\frac{4}{\varepsilon}+\frac{4}{\varepsilon^2}\\
&\quad -\frac{2}{\ln(1+\varepsilon)}-\frac{4}{\varepsilon\ln(1+\varepsilon)},\\
\langle\cos^3\theta\rangle &= \int_{-1}^{1} y^3\, f(y)\,\mathrm{d}y = 1+\frac{6}{\varepsilon}+\frac{12}{\varepsilon^2}+\frac{8}{\varepsilon^3}-\frac{8}{3\ln(1+\varepsilon)}\\
&\quad -\frac{8}{\varepsilon\ln(1+\varepsilon)}-\frac{8}{\varepsilon^2\ln(1+\varepsilon)}.
\end{aligned} \tag{2}$$

In equation (2) and throughout the paper angular brackets $\langle\,\rangle$ denote the average of a random variable.

The second type of collision considered in the examples is the Coulomb collision between charged particles. In this case the scattering angle is much smaller than in the electron-neutral collision. Using a classical model for Coulomb collisions, the PDF and the inverse CDF of the cosine of the scattering angle are [8, 14]:

$$f(y=\cos\theta) = \frac{\theta_{\min}^2}{2(1-y)^2} \Leftrightarrow \cos\theta = \frac{4R-\theta_{\min}^2}{4R+\theta_{\min}^2}, \tag{3}$$

where R is a random variable uniformly distributed between 0 and 1 and $\theta_{\min}$ the minimum scattering angle given by $|q_1q_2|/(2\pi\varepsilon_o m v^2\lambda_{De})$. Here q represents the charge of the colliding particles, ε_o the vacuum electrical permittivity, m the mass of the particle, v its velocity and λ_{De} the Debye length that is used as the maximum value of the impact

parameter. As a result of the screening of long-range interactions, $f(\cos\theta)$ is defined in the interval $[-1, \alpha]$ where $\alpha = (4-\theta_{\min}^2)/(4+\theta_{\min}^2)$. The averages of the first three powers of the cosine of the scattering angle are

$$\begin{aligned}
\langle\cos\theta\rangle &= \int_{-1}^{\alpha} y\, f(y)\,\mathrm{d}y = 1 - \frac{\theta_{\min}^2}{2}\ln\left(1+\frac{4}{\theta_{\min}^2}\right),\\
\langle\cos^2\theta\rangle &= \int_{-1}^{\alpha} y^2 f(y)\,\mathrm{d}y = \frac{1}{(4+\theta_{\min}^2)}\\
&\quad\times\left[4+5\,\theta_{\min}^2 - \theta_{\min}^2(4+\theta_{\min}^2)\ln\left(1+\frac{4}{\theta_{\min}^2}\right)\right],\\
\langle\cos^3\theta\rangle &= \int_{-1}^{\alpha} y^3 f(y)\,\mathrm{d}y = \frac{1}{(4+\theta_{\min}^2)^2}\left[16+40\,\theta_{\min}^2\right.\\
&\quad\left.+5\,\theta_{\min}^4 - \frac{3}{2}\,\theta_{\min}^2(4+\theta_{\min}^2)^2\ln\left(1+\frac{4}{\theta_{\min}^2}\right)\right].
\end{aligned} \tag{4}$$

3. Modelling the cumulative effect of N collisions

As particles undergo multiple collisions, they are randomly scattered and their final velocity and position must be described by random variables: the scattered angle after N collisions χ_N, the net axial displacement Δz_N and the off-axis displacements, Δx_N and Δy_N (or alternatively the radial displacement Δr_N and the azimuthal angle Φ_N). The PDFs of these random variables as a function of the number of collisions are in general complex and cannot be given by a closed-form expression. Exact analytical expressions for the PDFs can only be obtained as sums of series [5, 7]. Although a series expansion can capture the exact shape of a PDF, computing the series is not necessarily trivial or efficient from a practical point of view. In general, the coefficients of each expansion term are obtained by solving an integral and this integration can pose numerical challenges for high order terms (these terms are highly oscillatory). Furthermore, since many terms have to be considered in order to accurately capture the shape of the PDF, this approach is not efficient if the calculation has to be performed repeatedly.

An alternative approach is to assume that the distribution function after Ncollisions can be described by a function that belongs to a certain parametric family [8, 9]. In this case, one can approximate the PDF after Ncollisions by choosing a function from the parametric family such that the n first moments of the approximated distribution are the same as in the exact solution. Here n corresponds to the number of fitting parameters of the parametric family. The accuracy of this method depends on how well the parametric family can capture the shape of the real distribution function. Therefore, different collision types may require different parametric functions. Unlike in [8,9], no assumption is made in this work regarding the magnitude of the scattering angle of the real physical process. Therefore the results presented can be applied to any azimuthally symmetric collision.

The selection of the parametric functions should be based on expected characteristics of the real PDF. For the cosine of the scattering angle ($\cos\chi_N$), the parametric function must be monotonic and finite in the interval [−1,1], it should approximate a delta function ($\delta(1)$) when the number of collisions is zero ($N = 0$) and it should approximate a constant (0.5) when the number of collisions is very large ($N \to \infty$). It is also desirable that the parametric function reproduce the exact PDF of a single collision (equation (1) for elastic electron-neutral collisions or equation (3) for Coulomb collisions), so that no error is introduced when modelling only one collision ($N = 1$). One parametric family that fulfils these criteria is

$$\begin{aligned}
&\text{PDF}: \ f(\cos\chi) = \frac{A}{(1+B\cos\chi)^C},\\
&\text{CDF}^{-1}: \ \cos\chi = \frac{1}{B}\{R[(1+B)^{(1-C)} - (1-B)^{(1-C)}]\\
&\qquad +(1-B)^{(1-C)}\}^{1/(1-C)} - \frac{1}{B},\\
&\langle\cos\chi\rangle = -\frac{1}{B(2-C)} + \frac{1-C}{2-C}\frac{(1+B)^{(1-C)} + (1-B)^{(1-C)}}{(1+B)^{(1-C)} - (1-B)^{(1-C)}},\\
&\langle\cos^2\chi\rangle = \frac{1-C}{3-C} - \frac{2}{B\,(3-C)}\langle\cos\chi\rangle,
\end{aligned} \tag{5}$$

where A is a normalizing constant ($\int_{-1}^{1} f(\cos\chi)\mathrm{d}\cos\chi = 1$) and B and C are fitting parameters that depend on the number of collisions, N.

For comparison with [8], an exponential parametric family has also been considered for the case of Coulomb collisions:

$$\begin{aligned}
&\text{PDF}: \ f(\cos\chi) = A\exp(B\cos\chi),\\
&\text{CDF}^{-1}: \ \cos\chi = -1 + \frac{1}{B}\ln\{1 - R[1-\exp(2B)]\},\\
&\langle\cos\chi\rangle = \coth B - \frac{1}{B},\\
&\langle\cos^2\chi\rangle = 1 - \frac{2}{B}\langle\cos\chi\rangle.
\end{aligned} \tag{6}$$

Here A is again a normalizing constant and B a fitting parameter.

For describing statistically the particle displacements (Δ) in x, y (off-axis) and z (on-axis) directions, Gaussian distributions with mean μ and standard deviation σ have been considered:

$$\begin{aligned}
&\text{PDF}: \ f(\Delta) = \frac{1}{\sqrt{2\pi\,\sigma^2}}\exp\left(-\frac{(\Delta-\mu)^2}{2\sigma^2}\right)\\
&\text{CDF}^{-1}: \ \Delta = \mu + \sqrt{2\sigma^2}\,\mathrm{erf}^{-1}(2R-1).
\end{aligned} \tag{7}$$

In this work, we have favoured simplicity and clarity by selecting simple analytical expressions (equations (5)–(7)) as fitting parametric families. There is no reason, however, not to use alternative parametric functions. It is anticipated that using piecewise definitions of the PDFs will provide more flexibility and better accuracy. For example, the PDF of the axial displacement could be given by a Gaussian distribution of standard deviation σ_1 for $\Delta z > \mu$ and by a Gaussian distribution with standard deviation σ_2 for $\Delta z < \mu$.

3.1. Moments of the exact PDFs

The fitting parameters B, C, μ and σ in equations (5)–(7) are determined by forcing the parametric distributions of a particle undergoing N collisions to have the same first moments as the exact (unknown) PDFs. Therefore, expressions for the first moments of the exact PDFs are needed. Formulae to determine these moments as a function of the statistic of a single collision

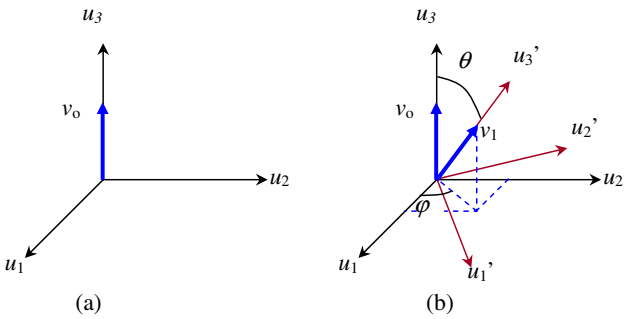

Figure 2. Coordinate system rotation following the scattering of the velocity vector after a single collision. (*a*) Before and (*b*) after the collision.

are developed in this section. For simplicity, it is assumed that the energy loss in a collision is negligible and therefore the N collisions have the same statistics. This is not too crude an approximation when considering Coulomb collisions or elastic collisions between particles of large mass difference. Treatment of energy loss will be addressed in section 4.2.

The cumulative scattering angle (χ_N) after N random collisions can be computed by tracking a particle as it undergoes each scattering event. Each collision results in a scattering of the incident particle by a polar angle, θ_i and an azimuthal angle, φ_i (figure 2). Following a derivation similar to that in [8], one can draw a coordinate system (u_1,u_2,u_3) such that the direction u_3 is aligned with the original velocity vector of the particle (figure 2). After the first collision, the velocity vector is scattered and a new coordinate system (u_1',u_2',u_3') can be drawn such that the new velocity and the new axis u_3' are again aligned. The relation between the two coordinate systems is given by a matrix rotation A_1 that accounts for the rotation by φ_1 and θ_1:

$$u = A_1 u' = \begin{bmatrix} \cos\varphi_1 \cos\theta_1 & -\sin\varphi_1 & \cos\varphi_1 \sin\theta_1 \\ \sin\varphi_1 \cos\theta_1 & \cos\varphi_1 & \sin\varphi_1 \sin\theta_1 \\ -\sin\theta_1 & 0 & \cos\theta_1 \end{bmatrix} \begin{bmatrix} u_1' \\ u_2' \\ u_3' \end{bmatrix}. \tag{8}$$

By construction, the columns of A_1 represent u_1', u_2' and u_3' in the previous (original) coordinate system. Similarly one can trace a new collision with respect to the last coordinate system by introducing a new matrix A_2. After N collisions,

$$u = A_1 A_2 \cdots A_N u^{(N)} = \begin{bmatrix} b_{11} & b_{12} & b_{13} \\ b_{21} & b_{22} & b_{23} \\ b_{31} & b_{32} & b_{33} \end{bmatrix} u^{(N)}. \tag{9}$$

The cumulative scattering angle (χ_N) is given by the angle between u_3 in the original coordinate system and $u_3^{(N)}$ in the last coordinate system, i.e. $\cos\chi_N = \vec{u}_3^{(N)} \cdot \vec{u}_3 = b_{33}$. In general, b_{33} is a complex function of φ_1, $\varphi_2, \ldots, \varphi_N$, θ_1, $\theta_2, \ldots, \theta_N$, all random variables. If the collisions are assumed to be azimuthally symmetric, i.e. $(1/2\pi)\int_0^{2\pi} \sin\varphi_i \, \mathrm{d}\varphi_i = (1/2\pi)\int_0^{2\pi} \cos\varphi_i \, \mathrm{d}\varphi_i = 0$, close form expressions for the first moments of $\cos\chi_N$ can be obtained (see appendices A and B):

$$\begin{aligned} &\langle\cos\chi_N\rangle = \langle\cos\theta\rangle^N, \\ &\langle\cos^2\chi_N\rangle = \frac{1}{3} + \frac{2}{3}\left(\frac{3}{2}\langle\cos^2\theta\rangle - \frac{1}{2}\right)^N, \\ &\langle\cos\chi_i \cos\chi_j\rangle = \left(\frac{1}{3} + \frac{2}{3}\left(\frac{3}{2}\langle\cos^2\theta\rangle - \frac{1}{2}\right)^i\right)\langle\cos\theta\rangle^{j-i}, \\ &\langle\cos^3\chi_N\rangle = \frac{3}{5}\langle\cos\theta\rangle^N + \frac{2}{5}\left(\frac{5}{2}\langle\cos^3\theta\rangle - \frac{3}{2}\langle\cos\theta\rangle\right)^N. \end{aligned} \tag{10}$$

Equation (10) links the (unknown) cumulative scattering angle after N collisions (χ_N) with the (known) scattering angle of a single collision (θ) (equations (2) and (4)). Equation (10) holds for any collision regardless of the amplitude of the scattering angle. The only constraint imposed in the derivation is that of azimuthal symmetry.

Regardless of the type of collision a particle undergoes, the net displacement of the particle in the axial direction after N collisions is given by

$$\begin{aligned} \Delta z_N = [&v_0 t_0 + v_1 t_1 \cos\chi_1 + v_2 t_2 \cos\chi_2 \\ &+ \cdots + v_{N-1} t_{N-1} \cos\chi_{N-1}]. \end{aligned} \tag{11}$$

where v_i is the particle speed after the ith collision, t_i the time between the ith and the $(i+1)$th collision and χ_i the scattering angle after the ith collision with respect to the initial velocity (figure 1). The particle is assumed to move with initial non-zero velocity v_o in the z (axial) direction ($\cos\chi_o = 1$). Equation (10) accounts for the axial displacement of the particle up to the Nth collision (figure 1).

Because the collisions are independent of each other, the time between collisions can be assumed to be given by an exponential distribution of mean $\langle t_i\rangle = \Delta t/N$. Combining equations (10) and (11) and noting that $\langle t_i^2\rangle = 2\langle t_i t_j\rangle = 2\langle t_i\rangle^2$, the moments of the PDF of the axial displacement are

$$\begin{aligned} \langle\Delta z_N\rangle &= \frac{v_o \Delta t}{N}\frac{1 - r^N}{1 - r}, \\ \langle\Delta z_N^2\rangle &= 2\left(\frac{v_o \Delta t}{N}\right)^2 \sum_{i=0}^{N-1} p_i \frac{1 - r^{N-i}}{1 - r}, \end{aligned} \tag{12}$$

where $r = \langle\cos\theta\rangle$ and $p_i = \langle\cos^2\chi_i\rangle$ are given by equations (2) (or (4)) and (10), respectively. The sum in equation (12) can be expanded but for conciseness the result is not presented here.

Collisions also result in particle diffusion in the off-axis direction (Δx, Δy). It can be shown that the displacement in the off-axis direction is characterized by

$$\begin{aligned} &\langle\Delta x_N\rangle = \langle\Delta y_N\rangle = 0, \\ &\langle\Delta x_N^2\rangle = \langle\Delta y_N^2\rangle = 2\left(\frac{v_o \Delta t}{N}\right)^2 \sum_{i=0}^{N-1} \langle\cos^2\Psi_i\rangle \frac{1 - r^{N-i}}{1 - r}, \\ &\langle\Delta r_N^2\rangle = \langle\Delta x_N^2 + \Delta y_N^2\rangle = 2\langle\Delta x_N^2\rangle, \end{aligned} \tag{13}$$

where Ψ_i is the angle between the velocity vector after the ith collision and the original x (or y) axis. Similarly to the derivation of equation (10), it can be shown that $\langle\cos^2\Psi_N\rangle$ as a function of the statistics of a single collision is given by

$$\langle\cos^2\Psi_N\rangle = \frac{1}{3}\left[1 - \left(\frac{3}{2}\langle\cos^2\theta\rangle - \frac{1}{2}\right)^N\right]. \tag{14}$$

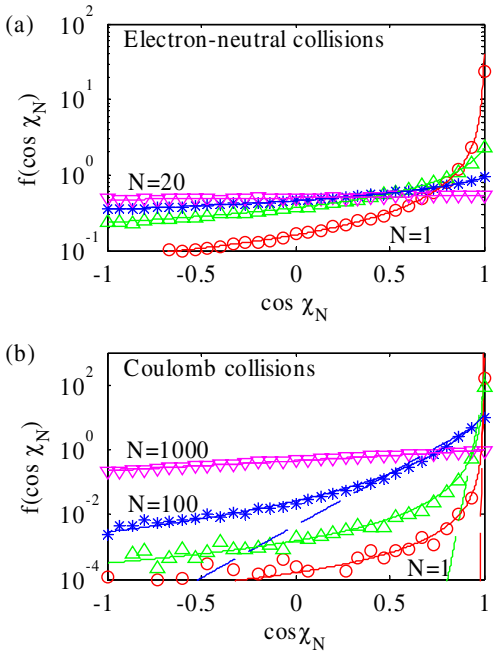

Figure 3. PDF of the cosine of the scattering angle after N collisions. Comparison between (symbols) PIC simulations in which each collision is modelled individually and (solid lines) the approximated distribution function obtained by fitting $f(x) = A/(1 + Bx)^C$ and enforcing the exact first moments. (*a*) Elastic scattering of 500 eV electrons with Ar neutrals. Distribution functions after $N = 1$, 3, 5 and 10 collisions (○, △, ∗ and ▽, respectively). (*b*) Coulomb scattering of electrons for $\theta_{\min} = 1°$. Distribution functions after $N = 1$, 10, 100 and 1000 collisions (○, △, ∗ and ▽, respectively). Dashed lines in (*b*) correspond to the fitting $f(x) = A\exp(Bx)$ as in [8].

3.2. *Exact versus approximated marginal PDFs*

Figure 3 shows various PDFs of the cosine of the scattering angle for a particle after it has undergone multiple collisions. A comparison between conventional PIC simulation results and the approximated PDF obtained by fitting a parametric function is presented. The PIC simulation results are obtained by tracking 5×10^5 particles as they undergo N collisions (each collision being modelled individually). Equation (5) is used as a parametric function to approximate the real PDF and the fitting constants B and C are calculated by forcing the approximated PDF to have the same first moments as the exact distribution (combining equations (5) and (10)). For comparison with [8], equation (6) has also been fitted for the Coulomb collision case. The new fit (equation (5)) has two fitting parameters which can be used to adjust the mean and variance of the approximated PDF simultaneously. On the other hand, equation (5) has only one fitting parameter and therefore it can only enforce the mean but not the variance. As a result equation (6) provides a better fit (figure 3(*b*)).

For a single parameter fitting curve, it is not possible to fit the variance of a real PDF once the mean has been fitted. It should be noted, however, that having two fitting parameters does not guarantee that the mean and variance of the real PDF can be reproduced. This is exemplified in figure 4. In this figure, the values of $\langle\cos\chi_N\rangle$ and $\langle\cos^2\chi_N\rangle$ that can be accessed with equation (5) are shown (clear area in the figure). Curves corresponding to N Coulomb collisions and

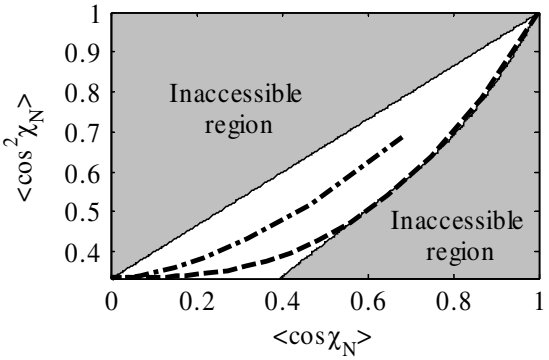

Figure 4. Accessible values of $\langle\cos\chi_N\rangle$ and $\langle\cos^2\chi_N\rangle$ for the parametric fitting $f(\cos\chi_N) = A/(1 + B\cos\chi_N)^C$. The shaded region cannot be accessed. The dashed line and the dash-dotted line correspond to the exact values of $\langle\cos\chi_N\rangle$ and $\langle\cos^2\chi_N\rangle$ for electrons undergoing multiple Coulomb ($\theta_{\min} = 1°$) and elastic collisions ($\varepsilon = 500$ eV), respectively.

N electron-neutral collisions are also presented. Since these curves fall in the area accessible by equation (5), close fits are possible. If the curves had fallen outside the accessible area, mean and variance could not be satisfied simultaneously. One can further elaborate the analytical PDFs (equations (5)–(7)) by introducing more parameters and increasing the number of moments that are satisfied. For the given examples, however, this seems unnecessary.

Gaussian fits (equation (7)) to the PDFs describing the on-axis and off-axis displacements are shown in figure 5. Although the fits conserve the mean and variance of the real PDF, the Gaussian fits of the particle displacement are not as accurate as the fits of the scattering angle. The error is larger when the number of collisions is small. A parametric family capable of reproducing the skewness of the real distribution would be preferable in this case.

The accuracy of multiple collision models is often measured by the error introduced in the first moments of distributions after one iteration. By this criterion, the present method introduces no error in the first two moments of the distributions and this accuracy is independent of the number of collisions modelled. This criterion, however, may not be the best way of measuring the accuracy. For example, it is clear that the fits to the PDF of the scattering angle (figure 3) are more accurate than those to the PDF of the axial displacement (figure 5), even though in both cases no error is introduced in the first two moments of the distributions.

One way of analysing the accuracy of the parametric fit is to quantify the error in high order moments. Computing high order moments, however, can be tricky and hard to interpret. Alternatively, the accuracy of the fit can be inferred by measuring the error induced in the first moments when simulating more than one iteration. If the fitted PDF did not introduce any error, the simulation result would not depend on the number of iterations required to model N_{total} collisions, i.e. one iteration accounting for $N = N_{\text{total}}$ collisions would give the same result as 10 iterations accounting for $N = 0.1N_{\text{total}}$ collisions per iteration. If the fitted PDFs are not exact, however, both simulations will yield different results.

Figures 6(*a*) and (*b*) compare the first moments of the cosine of the scattering angle obtained in PIC simulations with

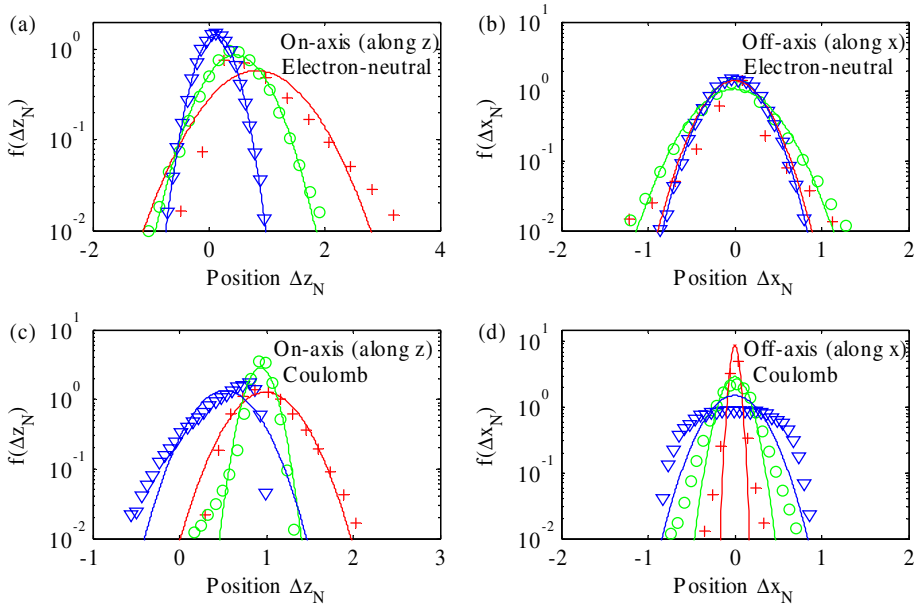

Figure 5. Gaussian fits to the PDF of the on-axis and off-axis displacements. Symbols represent the PDF obtained by simulating 5×10^5 particles (each collision individually) and solid lines the Gaussian fits. (*a*) On-axis and (*b*) off-axis displacement of 500 eV electrons undergoing elastic collisions with argon neutrals. Distribution functions after $N = 2$, 6 and 25 collisions (crosses, circles, and triangles, respectively); (*c*) on-axis and (*d*) off-axis displacement of electrons undergoing Coulomb collisions in a plasma where $\theta_{\min} = 1^\circ$. Distribution functions after $N = 10$, 100, 1000 collisions (crosses, circles and triangles, respectively).

those predicted by theory (equation (10)). The simulations tracked 5×10^5 particles as they underwent $N_{\text{total}} = 10^4$ collisions. Each simulation, however, modelled a different number of collisions (N) per iteration (see figure 6 for values of N). All the particles had initially the same position and velocity and the scattering angle in each iteration was obtained by sampling a fitted PDF given by equations (5) and (10). Figures 6(*a*) and (*b*) show that no significant error is introduced in the first moments of the scattering angle by simulating multiple collisions at a time. After N_{total} collisions, the same moments are obtained independently of the number of collisions modelled in one iteration. This agrees with the close fittings observed in figure 3.

Similarly, figures 6(*c*)–(*f*) compare the first moments of the axial position obtained in PIC simulations with those predicted by theory (equation (12)). The axial position was calculated accounting for the axial and radial displacements of the particles given by equations (7), (12) and (13). The average axial position $\langle z \rangle$ is accurately captured in the simulations independently of the number of collisions modelled in one iteration (figures 6(*c*) and (*d*)). $\langle z^2 \rangle$, however, can contain an appreciable error (figures 6(*e*) and (*f*)). Several remarks can be made in this respect. Independently of the number of collisions being modelled in one iteration, the first iteration always yields the right moments (including $\langle z^2 \rangle$). The error in $\langle z^2 \rangle$ as the simulation progresses beyond the first iteration is systematic, i.e. it cannot be attributed to statistical noise due to a limited number of particles. The resulting $\langle z^2 \rangle$ is always lower than the theoretical one. Since the slope of $\langle z^2 \rangle$ versus N_{total} is related to the diffusion constant, particle diffusion is systematically underestimated. And finally, this underestimation has its origin not only in the error introduced by the approximated PDF of the particle displacement (figure 5) but also in the correlation between the scattering angle and the particle displacement (see next section).

3.3. Correlation between variables: Gaussian copula

As shown in figures 3 and 5, the PDFs of the scattering angle and the displacement of a particle after it has undergone N collisions can be approximated by parametric functions (equations (5)–(7)) that provide the same first moments as the real PDF (equations (10), (12) and (13)). Sampling these distribution functions, however, must be done carefully because in general the variables are correlated. Therefore, the random numbers (R_1, R_2, ...) used for inverting each CDF cannot be independent.

Figure 7 shows the correlation between the scattering angle and the axial displacement as a function of the number of collisions. In this figure, the Pearson correlation factor (ρ_{p}) given by equation (15) and the Spearman rho (ρ_{s}) are compared. The Spearman rho measures the rank correlation [15, 16, 17] and its value was determined by post-processing conventional PIC simulation results:

$$\rho_{\text{p}_{\cos\chi,\Delta z}} = \frac{\langle \cos\chi_N \Delta z_N \rangle - \langle \cos\chi_N \rangle \langle \Delta z_N \rangle}{\sigma_{\cos\chi_N} \sigma_{\Delta z_N}}$$
$$= \frac{(v_0 \Delta t/N)[\sum_{i=0}^{N-1} p_i r^{N-i}] - \langle \cos\chi_N \rangle \langle \Delta z_N \rangle}{(\langle \cos^2\chi_N \rangle - \langle \cos\chi_N \rangle^2)(\langle \Delta z_N^2 \rangle - \langle \Delta z_N \rangle^2)}. \quad (15)$$

Expressions for all the terms in equation (15) have already been determined as a function of the statistics of a single collision. As one could expect, the correlation cannot be ignored. Although it tends to zero as the number of collisions increases, it does so very slowly. Even when the scattering angle is isotropic, a significant correlation between the angle and the position may still persist. For example, after 10 elastic electron-neutral collisions the scattering

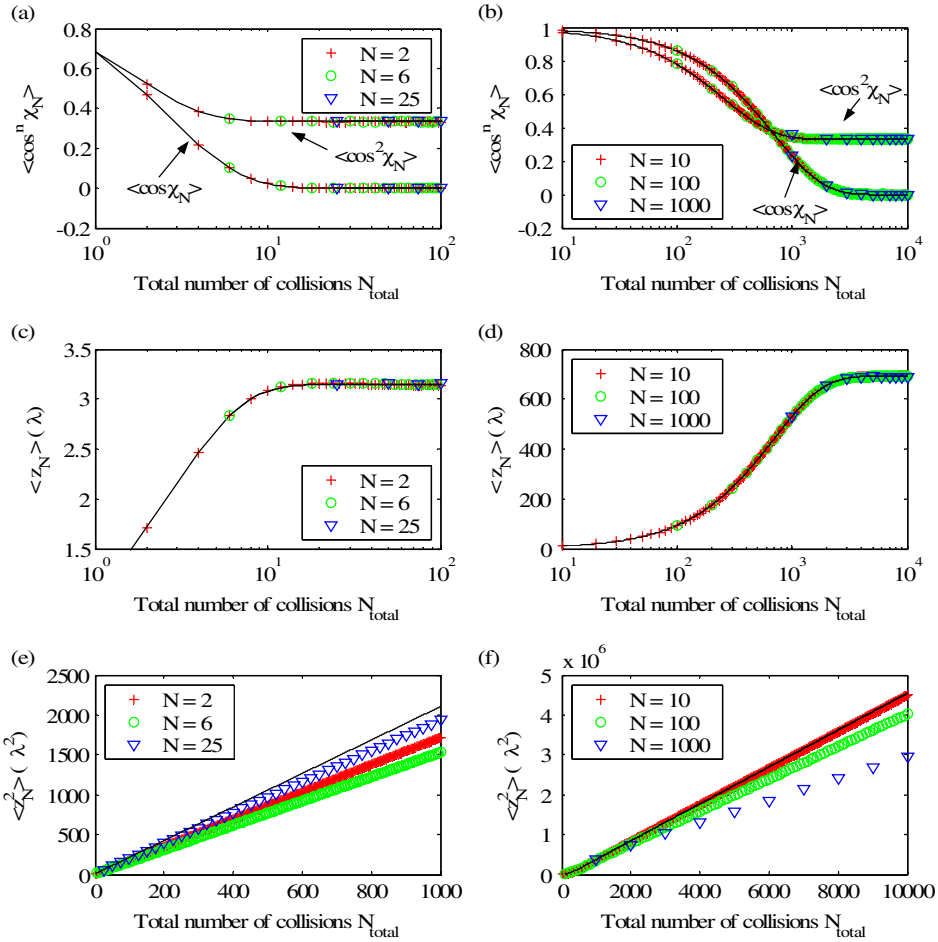

Figure 6. Comparison of the first moments of (*a*), (*b*) the scattering angle and (*c*)–(*f*) the particle position for various values of N (number of collisions modelled in one iteration). Symbols represent PIC simulation results for (*a*), (*c*), (*e*) electron-neutral collisions (500 eV electrons) and (*b*), (*d*), (*f*) Coulomb collisions ($\theta_{\min} = 1^\circ$). The black solid lines represent the theoretical values (equations (10) and (12)).

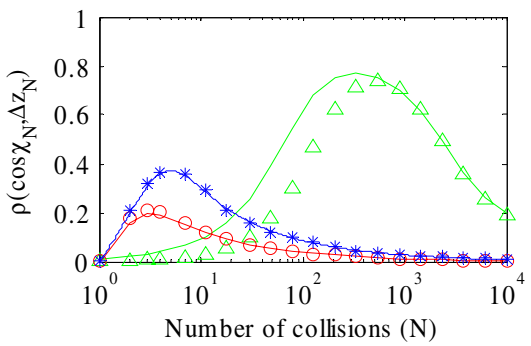

Figure 7. Correlation factor between the cosine of the cumulative scattering angle ($\cos\chi_N$) and the net axial displacement (Δz_N) as a function of the number of collisions (N). Straight lines correspond to the Pearson correlation factor ρ_p (equation (15)) and the symbols to the Spearman ρ_s obtained from a PIC simulation. Circles are for elastic scattering of 15 eV electrons in argon, stars for elastic scattering of 500 eV electrons in argon and triangles for electrons undergoing Coulomb collisions ($\theta_{\min} = 1^\circ$).

angle is close to isotropic (figure 3) but the correlation factor is still quite large (figure 7). For this particular example, only after $\sim 10^4$ collisions does the correlation approach zero.

Since $\cos\chi_N$, Δz_N, Δx_N and Δy_N are not independent, knowledge of the individual (marginal) distribution functions (or their approximations) is not sufficient for a complete statistical description. Instead, joint PDF is needed. Trying to fit the joint distribution by a simple analytical formula as has been done for the individual PDFs, however, seems unfeasible. Alternatively, one can use a copula [16] to join the marginal PDFs $f(\cos\chi_N)$, $f(\Delta x_N)$, $f(\Delta y_N)$ and $f(\Delta z_N)$ with a desired degree of correlation. Copulas are joint PDFs with uniform marginal distributions in [0,1]. Using copulas, a multivariate distribution can be constructed by specifying separately the desired marginal PDFs and their degree of correlation. The selection of the copula determines how the correlation takes place between the random variables. For example, some copulas emphasize more than others the coupling at the tails of the individual distributions. In this work a Gaussian copula is used for its physical representation of the correlation as well as its easy computation and possible generalization to multiple dimensions. Gaussian copulas are preferred for modelling linearly correlated variables and display symmetric correlation on both tails.

The Pearson correlation ρ_p (equation (15)) is a measure of the linear dependence of random variables and therefore it is not preserved in non-linear transformations. As a result,

the correlation between two random variables is not the same as the correlation between the two random numbers used for inverting the individual CDFs. It is therefore preferable to work with rank correlations (e.g. Spearman rho ρ_s) because they are preserved in non-linear monotonic transformations [18] such as the inversion of a CDF, i.e. the rank correlation between two random variables and that of the two random numbers used for inverting their CDFs are the same.

Determining analytically a relation between the Pearson correlation and a rank correlation for a given multivariate distribution is not always possible. For a multivariate Gaussian distribution, however, the following relation stands [17]:

$$\rho_p = 2 \sin\left(\frac{\rho_s \pi}{6}\right) \tag{16}$$

where ρ_p is the Pearson correlation factor and ρ_s the Spearman's rho.

Figure 8 shows a flow diagram of the steps needed to compute the scattering angle and the net displacement of an electron undergoing multiple collisions by means of a Gaussian copula. Given the electron energy, plasma conditions and number of collisions, a parametric fit is carried out by enforcing the correct first moments of the approximated individual PDFs. Since the Pearson correlation is not preserved by the copula, a rank correlation (e.g. Spearman rho) needs to be specified. This value can be pre-tabulated as a function of the electron properties. It turns out that for the elastic collisions, the Spearman rho and the Pearson correlation are close in value (see figure 7). Therefore in this case the rank correlation can be approximated by equation (15). Unfortunately, this is not always the case (see figure 7 for Coulomb collisions). The Gaussian copula is then constructed after determining the covariance matrix that will provide the desired rank correlation of the final variables. Samples of the multi-variate Gaussian are then inverted to obtain uniformly distributed random numbers (R_1, R_2, ...) with the desired rank correlation in between them. These numbers are then used for inverting the marginal CDFs.

It should be noted that the flow diagram in figure 8 is not necessarily the way a code implementation will look like. Several steps can be bypassed by using pre-tabulated data and if a marginal distribution of one of the variables is Gaussian, there is no need for inverting the sample of the Gaussian multivariate and then the marginal distribution. Instead, a simple renormalization of the samples will be a more efficient approach.

Figure 9 shows a comparison of the joint PDF (Δz_N, $\cos\chi_N$) obtained by means of a Gaussian copula (figures 9(*e*) and (*f*)) with the one obtained in a conventional PIC simulation where the collisions of 5×10^5 particles were treated individually (figures 9(*c*) and (*d*)). The joint PDF that results when the correlation between the scattering angle and the displacement is ignored is also shown for comparison (figures 9(*a*) and (*b*)). Accounting for the correlation by means of a Gaussian copula leads to a better approximation of the real joint distribution.

It was shown in section 3.2 that the accuracy of the method can be analysed by quantifying the error induced in the first moments of the distributions as the simulation progresses. The largest error is introduced in the slope of $\langle z_N^2 \rangle$ versus N_{total}, which results in an underestimation of the particle diffusion. In figure 10 the slope of $\langle z_N^2 \rangle$ versus N_{total} as a function of the number of collisions modelled in one iteration N is shown. The slopes are normalized by dividing the measured slope by the theoretical value, i.e. a value of 1 in figure 10 implies no error. Three cases, each with a different correlation between the scattering angle and the displacement, are plotted. The three cases are: no correlation (for the data displayed in figure 6), correlation imposed by a

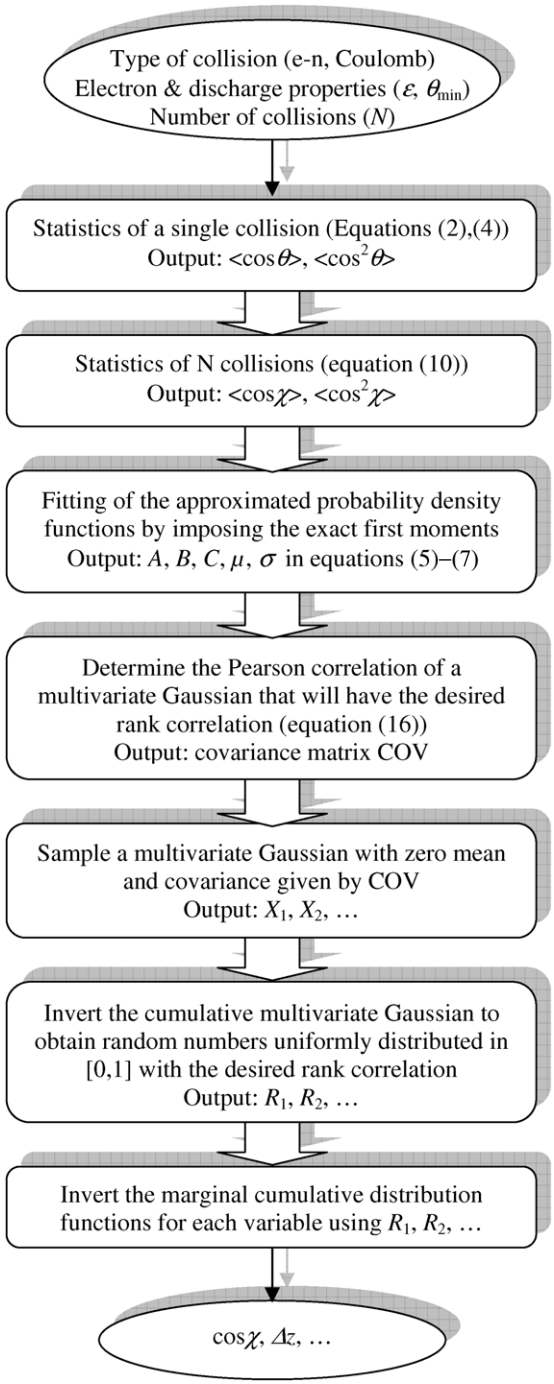

Figure 8. Flow diagram for computing the scattering angle and the net displacement of a particle undergoing multiple collisions. Correlation between the angle and displacement is enforced by a Gaussian copula.

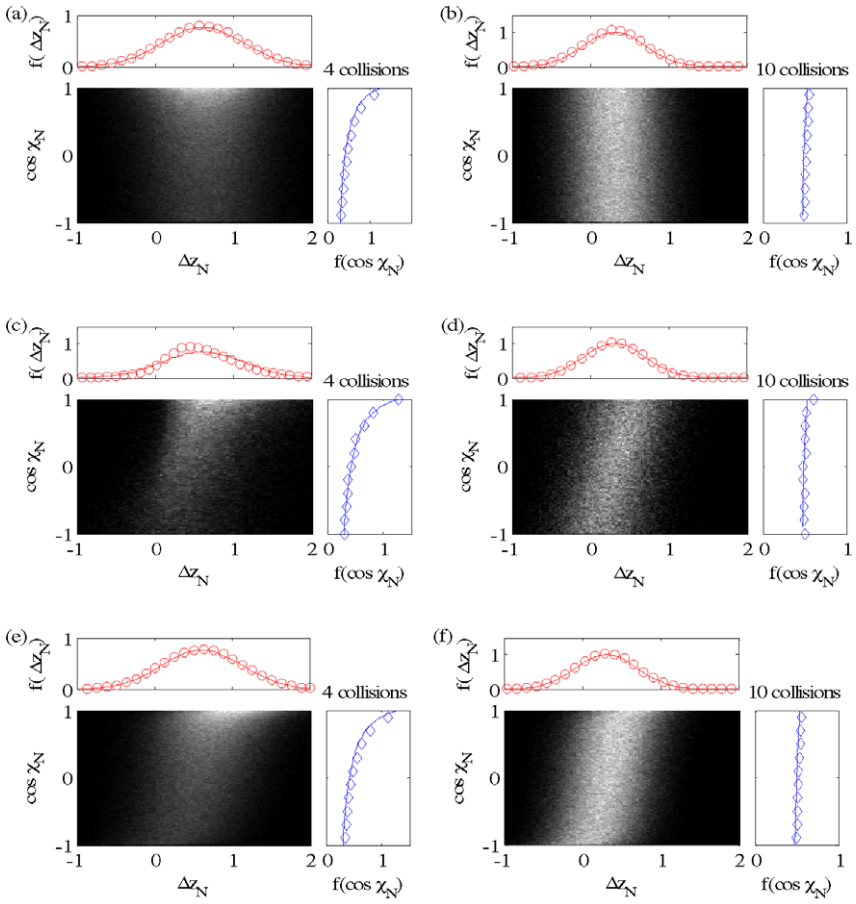

Figure 9. Comparison of joint PDFs (Δz_N, $\cos\chi_N$). (*a*) and (*b*) joint PDF obtained by fitting the marginal PDFs and ignoring correlation. (*c*) and (*d*) joint PDF obtained by tracking 5×10^5 particles in a conventional PIC simulation (each collision treated individually). (*e*) and (*f*) Joint PDF obtained by fitting the marginal PDFs and imposing correlation by means of a Gaussian copula. Distributions are shown after (*a*), (*c*) and (*e*) 4 electron elastic collisions with argon neutrals and (*b*), (*d*) and (*f*) 10 electron-neutral collisions for 500 eV electrons. Marginal PDFs computed from the joint distributions are shown with symbols and fitted marginal PDFs with solid lines.

Gaussian copula (as described in figure 8) and correlation equal to 1. It can be concluded that accounting for the correlation by means of a Gaussian copula reduces the error. Some error, however, still persists. The similar shape of the error (figure 10) and the correlation between the scattering angle and the displacement (figure 7) suggest that the correlation is not perfectly accounted for. It should be noted, however, that even if the correlation is forced to be 1, the diffusion constant is still underestimated for some values of N (figure 10). This indicates that at least part of the error is due to the inaccurate representation of the PDF of the particle displacement by a Gaussian profile (figure 5). Further analysis to determine the main contribution to the error and a comparison with other copulas and parametric families shall be carried out in the future.

Modelling multiple collisions in one time step accounting for the correlation between coordinates requires more computation than the treatment of a single collision. Therefore, multiple collision schemes are computationally interesting only if a sufficiently large number of collisions are modelled in one iteration. For an efficient implementation of the flow diagram shown in figure 8 with the marginal PDFs given by equations (5) and (7), the multiple collision scheme is computationally less expensive than the treatment of individual collisions when the number of collisions computed in one iteration (N) is larger than $\sim$10. This threshold number, however, depends on the parametric families and the copula used. Since the number of elastic collisions required for the electrons to relax their energy is of the order of $\sim 10^4$, even less efficient implementations can provide important computational savings.

4. Multiple collisions in plasma simulations

In section 3, a scheme was introduced for modelling N collisions without tracking each collision individually. The method approximates the PDFs of $\cos\chi_N$, Δx_N, Δy_N and Δz_N by parametric functions. By construction, the approximated PDFs have the same first moments as the real PDFs and the correlation between the variables can be enforced by means of a Gaussian copula. Although this model is more complete than others already used to study some typical plasma physics problems [8], refinements and new developments are needed to extend the applicability/accuracy of this technique to the simulation of low-temperature bounded plasmas. Some pending issues are discussed in this chapter and when possible we suggest possible improvements.

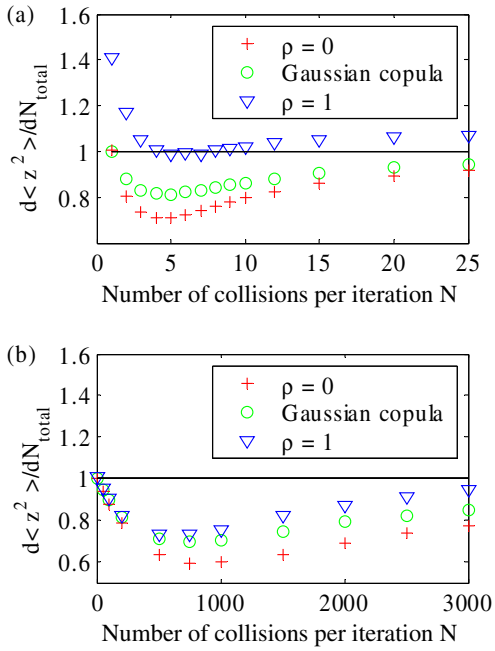

Figure 10. Slope of $\langle z^2 \rangle$ versus the total number of collisions (N_{total}) as a function of the number of collisions (N) modelled in one iteration (see figures 6(*e*) and (*f*)). Simulation results assuming three correlation factors between the scattering angle and the particle displacement are shown. The plots are normalized against the theoretical value so that 1 represents no error.

4.1. Cumulative effect of multiple collisions during a fixed time step Δt

Typical PIC simulations of bounded plasmas are performed by integrating the equations of motion in a fixed time step, Δt. Therefore, the application of the multiple collision scheme presented in section 3 requires pre-determining the number of collisions that a particle undergoes in a time step by sampling a Poissonian distribution. Since this has to be done at every time step and for each particle, it represents a significant computation cost. It is therefore desirable to obtain approximated PDFs for a particle undergoing multiple collisions in a fixed Δt without having to determine explicitly the number of collisions it undergoes. This would allow for a more efficient code by eliminating the need of sampling a Poissonian distribution before advancing each particle every time step. Note also that since Δt is fixed at the beginning of the simulation, variables that depend on Δt can be computed only once and easily stored at the beginning of the simulation (pre-storing data as a function of the number of collisions N, requires more space as N will have to be varied to cover a significant range). The PDFs after N collisions (section 3) and the PDFs after a fixed Δt are related:

$$g(\xi_{\Delta t}) = \sum_i P(N_{\text{collisions}} = i) f(\xi_i)$$
$$= \sum_i \left[\frac{(\nu \Delta t)^i}{i!} \exp(-\nu \Delta t) \right] f(\xi_i), \tag{17}$$

where ξ stands for either $\cos\chi$, Δx, Δy or Δz, $g(\xi)$ for the PDF after a time interval Δt, $f(\xi)$ for the PDF after N collisions and $P(N = i)$ is the probability of a particle undergoing $N = i$ collisions in Δt. This probability is given by a Poisson distribution of mean $\nu \Delta t$. Here $\nu = (n_g \sigma)^{-1}$ is the collision frequency. Moments of the new PDFs can be obtained combining equation (17) and previous results. For example,

$$\langle \cos\chi_{\Delta t} \rangle = \exp[-\nu\, \Delta t\, (1 - \langle \cos\theta \rangle)],$$
$$\langle \Delta z_{\Delta t} \rangle = \lambda \frac{1 - \langle \cos\chi_{\Delta t} \rangle}{1 - \langle \cos\theta \rangle}, \tag{18}$$
$$\langle \Delta z_{\Delta t}\ \cos\chi_{\Delta t} \rangle = \frac{\lambda}{3} \left[\frac{1 - \langle \cos\chi_{\Delta t} \rangle}{1 - \langle \cos\theta \rangle} + 4 \frac{\langle \cos\chi_{\Delta t} \rangle - \exp[-(3/2)\nu \Delta t (1 - \langle \cos^2\theta \rangle)]}{1 + 2\langle \cos\theta \rangle - 3\langle \cos^2\theta \rangle} \right],$$

where $\lambda = v_o/\nu$ is the mean free path of the particle. When determining the displacement of a particle undergoing N collisions in a fixed time interval Δt, the particles should be allowed to travel after the Nth collision provided that they do not collide again, i.e. the N^{th} collision can take place sometime before the end of the time interval Δt. This consideration requires trivial modifications of equation (11) and those derived from (11) (an additional term $v_N t_N \cos\chi_N$ should be included in equation (11)).

Although the average quantities for a fixed time step Δt (18) have been derived from a geometrical description of the particle motion, the same results can be obtained by solving the diffusion Boltzmann equation [4–7]. To model statistically the scattering angle and the net displacement of a particle undergoing multiple collisions in a time step Δt, one can proceed in the same way as for the case of N collisions. It only requires using the appropriate formulae for the moments of the exact PDFs.

In general, PDFs after a certain time interval Δt differ from those that account for N collisions even if the number of collisions N is set equal to the average number of collisions occurring in Δt, i.e. $N = \nu \Delta t$. Therefore, different parametric families may be chosen. A comparison between the average scattering angle for the two cases (fixed N and fixed Δt) is shown in figure 11. While no significant variation is observed for the case of small angle Coulomb collisions, a significant discrepancy is appreciable in the case of elastic electron-neutral collisions. Therefore, using equations derived in section 3 and setting $N = \nu \Delta t$ is only valid for collisions with a small scattering angle. Strictly speaking, however, this is not correct.

The leap-frog method is a popular choice for integrating the equations of motion in plasma simulations. This method is simple to implement, requires little memory and provides fast performance. The leap-frog method uses an interleaved representation where the external forces acting upon a particle and the particle position are known at times t_o, $t_o + \Delta t, \ldots$, while the particle velocity at times $t_o - 1/2\Delta t, t_o + 1/2\Delta t, \ldots$. This allows for a time-centred discretization of the equations of motion and yields second order accuracy. The implications of this interleaved representation when modelling multiple collisions falls beyond the scope of this paper. It is noted, however, that in the absence of an external force, the interleaved representation is not required because the particle position is determined statistically without integrating the particle velocity. This, however, may not be true in the presence of an external force. Since the current model does not consider external forces it is not possible to determine the implications of combining multiple collisions with this popular method for integrating the equations of motion.

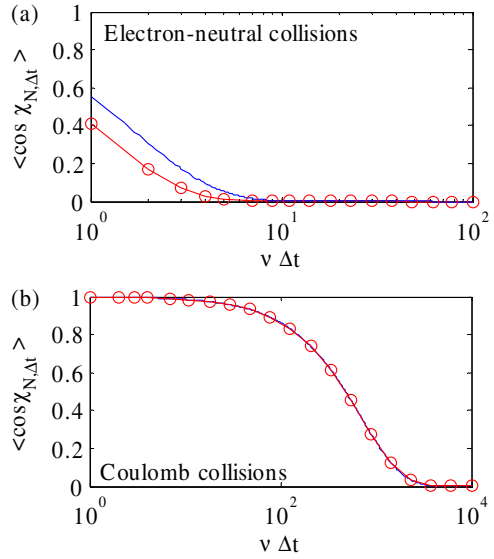

Figure 11. Comparison of (○) the mean scattering angle after N collisions $\langle \cos \chi_N \rangle$ and (——) the mean scattering angle after a given time step $\langle \cos \chi_{\Delta t} \rangle$ for (*a*) 15 eV electrons scattered in Argon and (*b*) electron undergoing Coulomb collisions with $\theta_{\min} = 1^\circ$. $N = \nu \Delta t$ is assumed for the comparison.

4.2. Energy exchange

So far it has been assumed that all the collisions a particle undergoes have the same differential cross section and that this cross section is determined by the initial particle velocity v_o. This implies that the scatterers are fixed in space and that the colliding particle does not lose energy in the collision, i.e. the magnitude of the relative velocity between the particle and the scatterer is always the same. Obviously this is not the case and collisions lead to energy exchange between the colliding particle and the scatterer. Assuming that the scatterers are still immobile, the relation between the velocity before (v_i) and after (v_{i+1}) an elastic collision is [14]

$$v_{i+1} = v_i \sqrt{1 - \frac{2m_1 m_2}{(m_1 + m_2)^2}(1 - \cos\theta_i)}, \qquad (19)$$

where θ_i is the scattering angle of the ith collision and m_1 and m_2 the particle and scatter masses. Ignoring the energy loss in a collision is not too crude an approximation if either the particle and the scatterer have very different masses (e.g. electrons and neutrals) or the scattering angle is small (e.g. Coulomb collisions). If the change in differential cross section due to the energy loss is negligible, the mean scattering angle of the colliding particle is not affected by the energy loss and equation (10) still holds. The particle position, however, needs to be adjusted. It is not difficult to show that for the energy loss given by equation (19), equation (12) is still valid if we let

$$r = \left\langle \sqrt{1 - \frac{2m_1 m_2}{(m_1 + m_2)^2}(1 - \cos\theta)}\cos\theta \right\rangle,$$

$$p_i = \frac{1}{3}\left\langle 1 - \frac{2m_1 m_2}{(m_1 + m_2)^2}(1 - \cos\theta)\right\rangle^i + \frac{2}{3}\left\langle \left(\frac{3}{2}\cos^2\theta - \frac{1}{2}\right) \times \left(1 - \frac{2m_1 m_2}{(m_1 + m_2)^2}(1 - \cos\theta)\right)\right\rangle^i. \qquad (20)$$

Energy loss has also been considered in condensed-history Monte Carlo simulations [3–7] and formulae for the moments of the distribution functions accounting for the energy loss in a continuous slowing down approximation have been obtained [19].

In low-temperature plasma simulations it is not always possible to assume that the scatterers are immobile. For example, electron-neutral collisions can be treated as if the neutrals were immobile because the electron temperature is typically orders of magnitude larger than the gas temperature. On the other hand, for coulomb collisions between particles of the same species, the particle and the scatterer have comparable speeds. For a significant number of particles, this can be treated using a statistically averaged scheme [8].

Another aspect to take into consideration is the presence of inelastic collisions. The straightforward solution is to apply the multiple collision scheme to particles that do not undergo inelastic collisions and to model each collision individually for the rest of the particles. In contrast with beam physics and condensed-history simulations, in typical low-temperature plasmas the vast majority of electrons are below the excitation and ionization thresholds. Therefore, even if high-energy electrons are tracked through each individual collision, the treatment of multiple collisions of the low-energy electrons will result in significant reduction of the computational cost. Combining infrequent inelastic and frequent elastic collisions in one time step can also be performed in a fashion similar to the 'hard'–'soft' collisions in condensed-history Monte Carlo simulations [5].

4.3. Electric field

All the theories of multiple collisions assume that no external forces other that those exerted by the scatterers act on the colliding particles. Therefore, these theories can be applied to charged particles only in the absence of external electric and magnetic fields. In low-temperature bounded plasmas, however, charged particles are constantly being accelerated by an applied electric field. Thus, it is desirable to develop a scheme to account for the multiple collisions and simultaneously for the field force.

Unfortunately, even if the force is assumed to be constant during the time step, modelling its effect on the particle scattering angle and net displacement is not trivial. An exact geometrical analysis as the one presented in section 3 becomes intractable as the electric field constantly changes the direction of the particle. One can think of the electric field as a virtual collision that accelerates/decelerates the particle and deflects it towards the direction of the field. These effects can be treated by introducing new rotation matrices in equation (9). The angles of these rotations, however, depend on the previous collisions of the particles and it is not azimuthally symmetric.

An analysis based on the solution of the Boltzmann equation using spherical harmonics (if the electric field and the initial particle velocity are not aligned the resulting distribution will not be azimuthally symmetric and an expansion on Legendre polynomials is not sufficient) well presents a known difficulty.

Modelling the multiple collisions in the presence of the electric field is therefore an area open for research.

5. Conclusions

A model for modelling the cumulative effect of multiple collisions in particle simulations has been presented. In contrast to other approaches where after one iteration the errors in the first moments of the distribution functions (scattering angle and particle displacement) depend on the number of collisions modelled, this model preserves the first moments independently of the number of collisions.

The model approximates the marginal PDFs of the final scattering angle and the particle displacement by parametric functions and enforces correlation by means of a Gaussian copula. The approximated PDFs have the same first moments as the exact distributions. This can be accomplished because formulae for the moments of the exact PDFs as a function of the statistics of a single collision can be derived. The formulae presented in this work hold for any azimuthally symmetric collision regardless of the amplitude of the scattering angle. Although in one iteration the first moments of the distributions are preserved, particle diffusion tends to be underestimated. This underestimation is attributed to the error introduced by the approximated distribution function of the particle displacement and the way correlation is established by the copula.

Multiple collision algorithms are computationally interesting only if a sufficiently large number of collisions are modelled simultaneously. The threshold number of collisions above which multiple collision algorithms become an interesting computational option depends on the parametric families used for approximating the real PDFs and the copula use to account for the correlation between variables. For the given examples, the presented multiple collision algorithm is an interesting choice when modelling more than ~10 collisions in one iteration.

Further improvements of the model have also been discussed. Multiple collision models have been very successful in the study of particle penetration and diffusion in matter. No multiple collision theory, however, has addressed modelling multiple collisions in the presence of an external electric field. Although not required for every application, taking into account the influence of an external field is necessary for implementing multiple collision models in low-temperature bounded plasma simulations. Despite this limitation, multiple collision algorithms can still be used in plasma physics to study some classical problems such as the thermalization of beams, moment and energy relaxation problems and temperature equilibration between various species.

Acknowledgments

This work was supported by the Korean Ministry of Science and Technology under the Tera-level Nano Devices Project—21C Frontier R&D Program.

Appendix A: analytical expression for determining $\langle \cos \chi_N \rangle$

The average scattering angle after N collisions (χ_N) can be obtained from equation (8) and (9). The cosine of the angle is given by the entry b_{33} in equation (9). For convenience this equation is reprinted here.

$$u = A_1 A_2 \cdots A_N u^{(N)} = \begin{bmatrix} b_{11} & b_{12} & b_{13} \\ b_{21} & b_{22} & b_{23} \\ b_{31} & b_{32} & b_{33} \end{bmatrix} u^{(N)}$$

$$\text{where } A_j = \begin{bmatrix} \cos\varphi_j \cos\theta_j & -\sin\varphi_j & \cos\varphi_j \sin\theta_j \\ \sin\varphi_j \cos\theta_j & \cos\varphi_j & \sin\varphi_j \sin\theta_j \\ -\sin\theta_j & 0 & \cos\theta_j \end{bmatrix}.$$

The scattering angle after $N = 1, 2, 3, \ldots,$ collisions are

$$\begin{aligned} \cos\chi_1 &= \cos\theta_1, \\ \cos\chi_2 &= \cos\theta_1\cos\theta_2 - \sin\theta_1\sin\theta_2\cos\varphi_1, \\ \cos\chi_3 &= \cos\theta_1\cos\theta_2\cos\theta_3 - \sin\theta_1\sin\theta_2\cos\theta_3\cos\varphi_1 \\ &\quad - \cos\theta_1\sin\theta_2\sin\theta_3\cos\varphi_2 + \sin\theta_1\sin\theta_3\sin\varphi_1\sin\varphi_2 \\ &\quad - \sin\theta_1\cos\theta_2\sin\theta_3\cos\varphi_1\cos\varphi_2, \\ \cos\chi_4 &= \cos\theta_1\cos\theta_2\cos\theta_3\cos\theta_4 + \cdots, \\ &\ldots, \end{aligned} \tag{A1}$$

where χ_N is the scattering angle after N collisions and (θ_i, φ_i) the scattering angles of the ith collision. Assuming that the collisions are azimuthally symmetric, we can average over φ_i to obtain from equation (A1)

$$\begin{aligned} \langle\cos\chi_1\rangle_\varphi &= \frac{1}{2\pi}\int_0^{2\pi} \cos\chi_1 \mathrm{d}\varphi_1 = \cos\theta_1, \\ \langle\cos\chi_2\rangle_\varphi &= \left(\frac{1}{2\pi}\right)^2 \int_0^{2\pi}\int_0^{2\pi} \cos\chi_2 \,\mathrm{d}\varphi_1\,\mathrm{d}\varphi_2 = \cos\theta_1\cos\theta_2, \\ \langle\cos\chi_3\rangle_\varphi &= \left(\frac{1}{2\pi}\right)^3 \int_0^{2\pi}\int_0^{2\pi}\int_0^{2\pi} \cos\chi_3 \,\mathrm{d}\varphi_1\,\mathrm{d}\varphi_2\,\mathrm{d}\varphi_3 \\ &= \cos\theta_1\cos\theta_2\cos\theta_3, \\ \langle\cos\chi_4\rangle_\varphi &= \left(\frac{1}{2\pi}\right)^4 \int_0^{2\pi}\int_0^{2\pi}\int_0^{2\pi}\int_0^{2\pi} \cos\chi_3 \,\mathrm{d}\varphi_1\,\mathrm{d}\varphi_2\,\mathrm{d}\varphi_3 \\ &= \cos\theta_1\cos\theta_2\cos\theta_3\cos\theta_4, \\ &\ldots, \end{aligned} \tag{A2}$$

where $\langle\ \rangle_\varphi$ denotes the average over φ. One can easily recognize a pattern and claim that

$$\langle\cos\chi_N\rangle_\varphi = \cos\theta_1\cos\theta_2, \ldots, \cos\theta_N. \tag{A3}$$

Since the scattering angles of each collision (θ_i) are independent, it follows that

$$\langle\cos\chi_N\rangle = \langle\cos\theta_1\rangle\langle\cos\theta_2\rangle\cdots\langle\cos\theta_N\rangle, \tag{A4}$$

where the brackets, $\langle\ \rangle$, indicate the overall average, i.e. over φ and θ. If all the collisions are assumed to have the same cross section, equation (A4) simplifies to equation (10) in the text.

To verify that equation (A4) is correct for an arbitrary number of collisions, N, the average value determined by (A4) can be compared with the average scattering angle obtained from a PIC simulation in which each collision is modelled individually. A comparison with a PIC simulation with 5×10^5 particles shows perfect agreement (within the noise of the particle simulation).

Appendix B: analytical expression for determining $\langle \cos^2 \chi_N \rangle$

The square of the cosine of the scattering angle after $N = 1, 2, 3, \ldots,$ collisions can be calculated from equation (A1).

$$\begin{aligned}
\cos^2\chi_1 &= \cos^2\theta_1,\\
\cos^2\chi_2 &= \cos^2\theta_1\cos^2\theta_2 - 2\sin\theta_1\sin\theta_2\cos\theta_1\cos\theta_2\cos\varphi_1\\
&\quad + \sin^2\theta_1\sin^2\theta_2\cos^2\varphi_1,\\
\cos^2\chi_3 &= (\cos^2\theta_1\cos^2\theta_2\cos^2\theta_3 - \sin\theta_1\sin\theta_2\cos\theta_3\cos\varphi_1\\
&\quad - \cos\theta_1\sin\theta_2\sin\theta_3\cos\varphi_2 + \sin\theta_1\sin\theta_3\sin\varphi_1\sin\varphi_2\\
&\quad - \sin\theta_1\cos\theta_2\sin\theta_3\cos\varphi_1\cos\varphi_2)^2,\\
\cos^2\chi_4 &= (\cos^2\theta_1\cos^2\theta_2\cos^2\theta_3\cos^2\theta_4 + \cdots)^2.\\
&\ldots,
\end{aligned} \tag{B1}$$

If the collisions are assumed to be azimuthally symmetric, averaging over the azimuthal angles φ_i leads to

$$\begin{aligned}
\langle\cos^2\chi_1\rangle_\varphi &= \frac{1}{2\pi}\int_0^{2\pi}\cos^2\chi_1\,\mathrm{d}\varphi_1 = \cos^2\theta_1,\\
\langle\cos^2\chi_2\rangle_\varphi &= \left(\frac{1}{2\pi}\right)^2\int_0^{2\pi}\int_0^{2\pi}\cos^2\chi_2\,\mathrm{d}\varphi_1\,\mathrm{d}\varphi_2\\
&= \frac{3}{2}\cos^2\theta_1\cos^2\theta_2 - \frac{1}{2}\sum_i\cos^2\theta_i + \frac{1}{2},\\
\langle\cos^2\chi_3\rangle_\varphi &= \left(\frac{1}{2\pi}\right)^3\int_0^{2\pi}\int_0^{2\pi}\int_0^{2\pi}\cos^2\chi_3\,\mathrm{d}\varphi_1\,\mathrm{d}\varphi_2\,\mathrm{d}\varphi_3\\
&= \frac{9}{4}\cos^2\theta_1\cos^2\theta_2\cos^2\theta_3 - \frac{3}{4}\sum_{i\neq j}(\cos^2\theta_i\cos^2\theta_j)\\
&\quad + \frac{1}{4}\sum_i\cos^2\theta_i + \frac{1}{4},\\
\langle\cos^2\chi_4\rangle_\varphi &= \left(\frac{1}{2\pi}\right)^4\int_0^{2\pi}\int_0^{2\pi}\int_0^{2\pi}\int_0^{2\pi}\cos^2\chi_3\,\mathrm{d}\varphi_1\,\mathrm{d}\varphi_2\,\mathrm{d}\varphi_3\\
&= \frac{27}{8}\cos^2\theta_1\cos^2\theta_2\cos^2\theta_3\cos^2\theta_4\\
&\quad - \frac{9}{8}\sum_{i\neq j\neq k}(\cos^2\theta_i\cos^2\theta_j\cos^2\theta_k)\\
&\quad + \frac{3}{8}\sum_{i\neq j}(\cos^2\theta_i\cos^2\theta_j) - \frac{1}{8}\sum_i\cos^2\theta_i + \frac{3}{8},\\
&\ldots,
\end{aligned} \tag{B2}$$

where $\langle\,\rangle_\varphi$ denotes the average over the azimuthal angle φ and the sums go from 1 to N. Although it is not as evident as for the case of $\langle\cos\chi_N\rangle$, one can identify a pattern in equation (B2) and claim that

$$\langle\cos^2\chi_N\rangle_\varphi = \frac{1}{3} + \frac{2}{3}\prod_{i=1}^{N}\left(\frac{3}{2}\cos^2\theta_i - \frac{1}{2}\right). \tag{B3}$$

Since the scattering angles of each collision (θ_i) are independent, it follows that

$$\langle\cos^2\chi_N\rangle = \frac{1}{3} + \frac{2}{3}\prod_{i=1}^{N}\left(\frac{3}{2}\langle\cos^2\theta_i\rangle - \frac{1}{2}\right), \tag{B4}$$

where the brackets, $\langle\,\rangle$, indicate average over φ and θ. If all the collisions are assumed to have the same cross section, equation (B4) simplifies to equation (10) in the text.

A comparison between $\langle\cos^2\chi_N\rangle$ given by (B4) and $\langle\cos^2\chi_N\rangle$ calculated from the results of a PIC simulation with 5×10^5 particles validates the equation.

The same approach followed to calculate $\langle\cos\chi_N\rangle$ and $\langle\cos^2\chi_N\rangle$ can be followed to determine $\langle\cos\chi_i\cos\chi_j\rangle$ and $\langle\cos^3\chi_N\rangle$. The final results are presented in equation (10).

References

[1] Hockney R W and Eastwood J W 1988 *Computer Simulation using Particles* (Bristol: Institute of Physics)
[2] Kim H C, Iza F, Yang S S, Radmilović-Radjenović M and Lee J K 2005 *J. Phys. D: Appl. Phys.* **38** R283
[3] Berger M J 1963 Monte Carlo calculation of the penetration and diffusion of fast charged particles *Methods in Computational Physics* vol 1, ed B Alder *et al* (New York: Academic) p 135
[4] Lewis H W 1950 *Phys. Rev.* **78** 526
[5] Fernandez-Varea J M *et al* 1993 *Nucl. Instrum. Methods* **B73** 447
[6] Kawrakow I and Bielajew A F 1998 *Nucl. Instrum. Methods* **B134** 325
[7] Kawrakow I and Bielajew A F 1998 *Nucl. Instrum. Methods* **B142** 253
[8] Nanbu K 1997 *Phys. Rev.* E **55** 4642
[9] Nanbu K and Yonemura S 1998 *J. Comput. Phys.* **145** 639
[10] Bobylev A V and Nanbu K 2000 *Phys. Rev.* E **61** 4576
[11] Birdsall C K and Langdon A B 1985 *Plasma Physics via Computer Simulation* (New York: McGraw-Hill)
[12] Vahedi V and Surendra M 1995 *Comput. Phys. Comm.* **87** 179
[13] Surendra M, Graves D B and Morey I J 1990 *Appl. Phys. Lett.* **56** 1022
[14] Lieberman M A and Lichtenberg A J 2005 *Principles of Plasma Discharges and Materials Processing* 2nd edn (New York: Wiley)
[15] Press W H, Flannery B P, Teukolsky S A and Vetterling W T 1992 *Numerical Recipes in C: The Art of Scientific Computing* (Cambridge: Cambridge University Press)
[16] Nelsen R 1999 *An Introduction to Copulas (Springer Lecture Notes in Statistics)* (Berlin: Springer)
[17] Kruskal W H 1958 *J. Am. Stat. Assoc.* **53** 814
[18] Dall'Aglio G, Kotz S and Salinetti G 1991 *Advances in Probability Distributions with Given Marginals* (Dordrecht: Kluwer)
[19] Sempau J, Wilderman S J and Bielajew A F 2000 *Phys. Med. Biol.* **45** 2263